Normal modes of a medieval tower excited by ambient vibrations in an urban environment

Andrea Morelli*[1], Lucia Zaccarelli[1], Adriano Cavaliere[1], and Riccardo M. Azzara[2]

[1]*Istituto Nazionale di Geofisica e Vulcanologia — Sezione di Bologna, Via Marcantonio Franceschini 31, 40135 Bologna, Italy.*

[2]*Istituto Nazionale di Geofisica e Vulcanologia — Sezione Roma 1, Osservatorio di Arezzo, Via Francesco Redi 13, 52100 Arezzo, Italy*

September 10, 2021

Declaration of Competing Interests: The authors acknowledge there are no conflicts of interest recorded.

*Corresponding author: andrea.morelli@ingv.it

Abstract

We report on a passive seismic experiment on a historical tower in northern Italy. Assessment of dynamical properties of such structures is known to be very important to anticipate their response to possible earthquake excitation. We show how classical seismological analyses can image, in high definition and detail, many modes of vibration, continuously excited by background tremor due to vehicle traffic. Similarly to what Earth's normal modes reveal, such information pose constraints on the elastic (and anelastic) structure of a building that, in the case of a historical edifice, are not generally known because appropriate information on its fabrication and constitution is not available. Our case refers to the XII-century, 97-meter tall, Asinelli tower in Bologna (northern Italy) — the tallest slender masonry building in Europe. We detect and analyze several modes of free flexural vibration, besides compressional and torsional modes. Free vibrations occur with slightly different natural frequencies along two orthogonal directions, as a consequence of a discrepancy between centers of mass and stiffness. This is apparent by the splitting of frequencies of modes of vibration. For each mode, the polarization of particle motion shows that energy cyclically transfers between the two different degrees of freedom of the system. The spectral signature of the nearby Garisenda tower can also be recognized on the spectrum of Asinelli, and vice-versa, but the frequencies differ so there is no cross influence between the two. These data can be used to calibrate the parameters used for dynamic modelling, to investigate variations in time of the dynamic response, and to characterize the anthropogenic sources of ground motion to possibly mitigate their effects. While the engineering community has extensively addressed the field of structural health monitoring with specific tools, we show that methods part of any seismologist toolbox can also provide detailed information about buildings, that can be used for their numerical modelling.

Introduction

The study of the normal modes of free oscillation of the Earth (e.g., Backus and Gilbert, 1961; Dziewoński and Gilbert, 1972, 1973; Gilbert and Dziewoński, 1975; Ritzwoller et al., 1986; Woodhouse et al., 1986; Deuss et al., 2013) is a classical topic in seismology, that has

produced remarkable results for the study of deep Earth structure (e.g., He and Tromp, 1996; Deuss et al., 2010; Ritsema et al., 2011), calculation of synthetic seismograms (Masters et al., 2011), and seismic source inversion (Gilbert and Dziewoński, 1975; Dziewoński et al., 1981; Ekström et al., 2012). Normal mode analysis is in fact a well-known and standard tool in many fields, among which acoustics, study of mechanical and electrical systems, structural dynamics, optics. Seismological approaches have been applied to different scales and environments, and even to the apple industry to quantify fruit firmness (van Wijk and Hitchman, 2017). Analysis of free vibrations a building, excited by distant earthquakes or ambient noise, is also effective as a tool to assess the response of the construction to stronger ground motion, with a goal of evaluating its seismic vulnerability (e.g. Clinton et al., 2006; Crowley and Pinho, 2010). It has been long used by the engineering community to obtain information about structures (e.g. Chopra, 2012; Taranath, 2012; Au, 2017). Information deriving from modal identification can be used to cast an inverse problem (in a process known in engineering as structural system identification) aimed at determining the structural properties of a system (e.g. Au, 2017). The response of a building even to small-amplitude excitation depends on — and, hence, gives information about — its elastic and anelastic properties. Such knowledge holds particular interest for historical buildings, for which little is known about construction details, and that are particularly susceptible to seismic damage. It may be used to constrain numerical full dynamic structural analyses (e.g. Peeters and De Roeck, 1999; Gallipoli et al., 2010; Prieto et al., 2010; Kaya and Şafak, 2015; Invernizzi et al., 2019; Azzara et al., 2020). We set our attention on a medieval monumental masonry tower in Bologna, Italy, where we aim to apply classical seismological techniques to measure free oscillations excited by urban ambient noise in a seismic monitoring campaign carried on for six months.

Determination of the response of buildings to ground motion is an important element to estimate the possible effects of seismic shaking, and hence structural vulnerability to earthquakes (Crowley and Pinho, 2010). Time-lapse monitoring is useful to monitor the state of health of constructions (Trifunac et al., 2001a,b). Analyses of seismic waves in buildings have indeed been the subject of many studies. Amplitude and apparent free fre-

quency changes with time (detected for earthquake shaking and ambient vibration tests) have been used to show that the response of a building and ground coupling depend on amplitude of excitation at the ground (e.g. Trifunac et al., 2001a,b). Using interferometric methods that take advantage of time domain transfer function approaches it has been shown that building response can be isolated from the excitation and soil-structure interaction by deconvolution of displacement recorded at different levels in the building (e.g. Snieder and Şafak, 2006; Kohler et al., 2007; Prieto et al., 2010) using either earthquake data and background noise (e.g. Prieto et al., 2010; Nakata et al., 2013; Nakata and Snieder, 2013). Waves can be identified propagating in densely instrumented buildings and modeled by means of models based on structural drawings (e.g. Kohler et al., 2007; Wu et al., 2021). The anisotropic behavior of buildings has also been imaged (Thompson and Snieder, 2006). Identification of modes of vibration of a structure under unperturbed conditions (ambient excitation) is the subject of operational modal analysis (OMA), a technique sometimes applied to complex buildings and high instrument densities to understand the impact of sources of excitation and following response of the structure (Au, 2017; Sarlo et al., 2018; Zhu et al., 2018). The natural excitation technique (NExT) is another method to identify the natural frequencies and mode shapes of a linear dynamic system using the measured output response of the system to a broadband (i.e., white noise) input excitation (e.g., James et al., 1995). We are however here interested in carrying on our analysis using rather classical methods and concepts taken from the study of normal modes of the Earth.

For historical buildings, vibrational analysis is particularly important as it may yield information useful to derive structural information, that is otherwise not known in detail (e.g. Riva et al., 1998; Casolo et al., 2013; Valente and Milani, 2016; Invernizzi et al., 2019). Asinelli and Garisenda — located in the city center — represent the most famous landmark for the city of Bologna. Taller Asinelli is known in science history because of experiments with falling bodies for early measurements of g by Giovanni Battista Riccioli, ca. 1650 (Graney, 2012), and calculation of earth rotation by Giovanni Battista Guglielmini in 1791 (Mantovani, 2019). The Two Towers (as Asinelli and Garisenda are commonly known) are

essentially tall, hollow, square-base prisms (Palermo et al., 2015; Invernizzi et al., 2019). Taller Asinelli, perhaps the tallest masonry building in Europe (and certainly the most slender), was built between 1109 and 1119. It is 97 m high, leans with an overhang of 2.2 m. Garisenda shows a more serious overhang of 3.2 m with a height of just 48 m after being cut down after its construction was interrupted because of settlement of foundations. Deformation of the Two Towers is continuously monitored by a permanent system, but no measure of vibrations is systematically recorded. A temporary campaign was therefore carried on from September 2013 to April 2014, consisting of a number of three-component seismometers installed at different levels inside the buildings, with the goal of studying dynamical response to background excitation, mainly ascribable to vehicular traffic. We have thus been able to observe and measure the oscillations of the two towers due to ambient noise and distant earthquakes.

[Figure 1 about here.]

In this paper, we show classical normal mode, or eigenvalue, analysis, using Fourier spectra and the multitaper spectral analysis technique (Prieto et al., 2009), applied to seismographic data recorded at different floors of the Asinelli tower. We first describe the field data collection, and the main features of the background noise field in the city center. We then report on the identification of frequencies of a number of natural modes of vibration of the building, and on the description of distinctive features of such modes. We conclude with a discussion on the impact of our observations on dynamical modeling and further developments with engineering interest.

Data acquisition

For this study, we installed, at 5 different levels inside the tower, three-component seismographic stations (Lennartz Le3D/5s velocity sensors, with 0.2 Hz eigenfrequency, RMS noise below 1 nm/s at 1 Hz, and 140 dB dynamic range; coupled with 24-bit RefTek digitizer and data acquisition systems, with sampling frequency set at 200 *sps*). A station has been positioned at street level just outside the building, others on external walls on

stone ledges, such as in windows, at approximate heights of 35, 55, 70 and 90 m (Figure 1). The building, with masonry walls (and rubble stone fill in the bottom sectors), is hollow with wooden stairs and decks inside (e.g., Palermo et al., 2015), so that seismometer installation had to follow architectural constraints and be limited by availability of proper stone sills. Two additional stations were set, for a shorter period of time, at the top level, at opposite corners of the terrace, to record torsional motions as explained in the following. Field activities have actually taken place indoors, but involved many climbs on wooden staircases and ladders. The instruments were kept recording continuously for about 6 months between September 20, 2013, and April 10, 2014. During this time, no local earthquakes have been recorded, so seismic traces mainly consist of the free vibrations of the building excited by background noise and occasional teleseisms. Recorded noise amplitudes typically increased in the central hours of the day, roughly from 9 am to 5 pm, coherently with the assumption of its anthropic origin due to traffic (Figure S1 in the electronic supplement to this article shows traces for the first 100 days of the field experiment).

Figure 2 shows one typical day of data, in 1-hour intervals starting from the midnight, recorded by the N component of the station installed at the top (AS97). Typically, noise records show amplitudes modulated by the hour of day: amplitudes increase in the central hours of the day (8 to 17, see also Figure S1 in the electronic supplement). This pattern is coherent with noise generated by anthropic activities and vehicular traffic, more intense in the central part of the day than in the early morning or late afternoon. In this record, referring to a Saturday, we note that noise actually reaches its maximum during the night (from 8 p.m. to 1 a.m.) when traffic restrictions in the city center are removed. Such a time dependence of noise amplitude clearly points to vehicle traffic as the source of excitation.

[Figure 2 about here.]

Increasing the time resolution, we can easily identify the existence of a clear and coherent flexure of the tower. Figure 3 shows 60 seconds of typical data, that reveal the

presence of a modulated oscillation with a period of approximately 3 s, very small at the base station (AS00) but gaining progressively higher amplitude going up along the tower (stations AS35, AS55, AS70, AS97). Note that the oscillation stays in phase at the different stations. This behavior is hence consistent with the presence of resonance in the building, excited by ambient vibrations such as due to traffic. The tower swings similarly to a shaken cantilevered beam. This is quite predictable and expected, but the pattern is so clear that it can plainly be identified even in the time domain. In the next section we show that spectral analysis can identify different modes of free vibration with high detail.

[Figure 3 about here.]

A mode catalog

We identify and characterize here a number of free modes of vibration of Asinelli, that portray its dynamic behavior, and represent constraints on its structure. The spectrum of ground acceleration, even with a quick calculation of plain Fourier transform for one day of data only, immediately reveals the presence of several resonant peaks (Figure 4) that identify the frequencies of different modes of free oscillation of the tower. The spectrum is clear with one day only of data, and it is very consistent over the whole 6-month period for which we have data. We are not able to detect significant wander of resonant frequencies in time.

[Figure 4 about here.]

A tall, slender building, such as a tower, can — to the first order — be seen as a cantilever beam (e.g. Taranath, 2012), and the existence of different modes of oscillations can be understood through the elementary Euler-Bernoulli, or the more widely used Timoshenko (that also includes transverse shear), beam models (e.g., Dym and Williams, 2007). The transverse displacement for the n-th mode, w_n, of an elementary uniform cantilevered beam (i.e., fixed at one end and free at the other) subject to flexure is given

in its simplest form by (Dym and Shames, 2013):

$$w_n = A\left[\cosh\beta_n x - \cos\beta_n x + \frac{(\cos\beta_n L + \cosh\beta_n L)(\sin\beta_n x - \sinh\beta_n x)}{\sin\beta_n L + \sinh\beta_n L}\right] \quad (1)$$

where x is distance along a beam of length L, β_n are the roots of:

$$\cosh(\beta_n L)\cos(\beta_n L) + 1 = 0$$

and A is a constant determined by initial conditions at $t = 0$ (that we can set to 1 for the sake of plotting mode shapes). Mode shapes for this case are shown in Figure 5. This is of course only a strong simplification. The building, dating back to the XII century, has wall thickness decreasing with height, irregularities, likely heterogeneous properties and defects, faulty foundations and subject to gravity with a verticality flaw. We will later on refer to accurate, numerical modelling of the actual tower (Invernizzi et al., 2019). However, we can now be conveniently guided by the simple solution of equation 1 to identify modes related to the natural resonance frequencies seen in Figure 4, that will be confirmed by the realistic numerical calculations. We identify the tallest, and gravest, peak with the fundamental mode, i.e. the main resonance also apparent in the time series (Figure 3). As expected, amplitudes increase from the ground-level station AS00 — bottom black line, barely showing a broad spectral peak, about 50 dB below the maximum — only marginally influenced by the resonance pattern of the tower. Stations located on the tower (AS35, AS55, AS70, AS97) understandably show amplitudes gradually increasing with elevation. The second peak, at about 1.3 Hz, refers to the second flexural mode, or first overtone, that we expect to have a nodal point almost at 0.8 times the length of the beam (Figure 5). In fact, the spectral amplitude of AS70 in Figure 4 is much smaller than the others, while amplitudes at the other stations are comparable (AS97, at the top, is still maximum). We can understand this feature, by looking at the shape of mode 2 (dashed line in Figure 5) that has a node below 0.8 times the length of the beam, and comparable amplitudes at 0.35 and 0.5 times the length. At higher frequency, there is a narrow but somewhat anomalous peak at 2.3 Hz, where the largest amplitude refers to AS70, that we will comment later on. We find another peak at about 3.3 Hz that we claim corresponds to the third flexural mode, and another

at about 5.5 Hz in agreement with a fourth flexural mode. This intuitive association of frequencies to flexural modes is confirmed by the detailed numerical analysis by Invernizzi et al. (2019). Although sophisticated methods are used in engineering for this purpose (such as Operational Modal Analysis, Au (2017)), and we only have few points along the tower, we can plot the spectral amplitudes for the different modes as retrieved for all the stations, to gain an idea of mode shapes (Figure 6).

[Figure 5 about here.]

[Figure 6 about here.]

Note that at about 0.7 Hz a small but clear peak (labeled G in Figure 4) is noticeable at street-level station AS00, but not at the others. As this peak is absent from the stations positioned along the tower, it is not compatible with free vibration of Asinelli, but is rather connected to ground motion that attenuates with elevation along the structure. We can recognize that it in fact corresponds to the frequency of the fundamental mode of nearby Garisenda, that we have identified in ground motion at decametric distance around the foundations (Azzara et al., 2014). It is well known that tall buildings, actively excited, can induce large dynamical forces in the ground, and related motion can be measured at distances up to few kilometers (Jennings, 1970), but even the smaller motions due to response to ambient noise can be measured around the buildings (Castellaro and Mulargia, 2010; Mucciarelli et al., 2017). Similarly, some of the modes of Asinelli can be recognized at the base station of Garisenda. Being resonance frequencies of the two towers different, there is luckily no interplay between the two structures: a common resonance frequency could be detrimental in the case of large shaking produced by earthquakes.

Finally, inspection of Figure 4 shows the interesting feature that resonance frequencies do not exhibit single peaks, but, rather, they are split (see the first two modes at about 0.3 Hz and 1.3 Hz). The splitting of frequencies of normal modes of free vibration is well known to seismologists, as it places important constraints on heterogeneous structure of the Earth's mantle and core (e.g. Woodhouse et al., 1986; Ritzwoller et al., 1986; Deuss et al., 2013). The free vibration responses of buildings can be quite diversified and

complex. It is in general possible that the twin, close, frequencies may be due to coupling between two principal directions, coupling between translational and torsional modes, beating, short-term meteorological effects including temperature variations or level of soil moisture. As we will however see with more detail in the following, all the main peaks (that we have associated to flexural modes of oscillation) share similar split behaviour. Besides, the slender, tall, tower is known to have significant inhomogeneities, in part due to construction, in part due to later damage, repair and modifications (e.g., Palermo et al., 2015). We may infer, then, that we are looking here at the effect of some departure from (axi-)symmetry, from the fact that frequency splitting is known to be linked to defects of symmetry in buildings (Trombetti and Conte, 2005), and on the basis of analysis of results of realistic finite element modelling (Invernizzi et al., 2019), that recognizes that bending results in slightly different natural frequencies in two orthogonal directions because of asymmetry of the tower.

To map mode frequencies with higher accuracy, and address the splitting of resonant frequencies in more detail, we use multitaper spectrum analysis (Thomson, 1982; Prieto et al., 2009), a classical technique often used for its ability to isolate single frequencies within noise. We also rotate components to find the principal directions that isolate separate spectral peaks (as shown in Figure S2 in the electronic supplement to this article). The result is shown in Figure 7 for the first two flexural modes, and in Figure 8 for the third mode. Principal directions are not the same for the first two modes, a rotation by 46° is required for Mode 1, while Mode 2 requires a rotation by -10°. Principal directions for Mode 3 almost coincide with cardinal directions N and E (Figure 8).

[Figure 7 about here.]

[Figure 8 about here.]

Particle motion for the different modes can be extracted by filtering horizontal component seismograms in the proper frequency bands (Figures 9, 10). Motion on the horizontal plane corresponding to the lowest-frequency spectral peak follows a polarization pattern oriented along the two principal directions already noted before, rotated 46° with respect

to the North (Figure 9, top). The pattern is typical for an oscillator with two degrees of freedom, where energy alternates between the two degrees of freedom. Plotting separately the oscillations along the two principal directions (Figure 9, bottom) shows such transfer of energy between the two directions. This behavior is known to exist for one-storey eccentric systems (Trombetti and Conte, 2005). Horizontal particle motion for higher modes is more complex (Figure 10). Mordret et al. (2017) found a main resonance peak for a high-rise building made of distinct peaks, but only along one of the two orthogonal building principal directions, with three split peaks that correspond to bilinear behavior such as due to breathing cracks (Chu and Shen, 1992). They infer that the origin of such behaviour may be located where displacement, corresponding to the only mode showing the phenomenon, is maximum, hence affecting this specific mode more than others. Although the process we are seeing is not related to bilinear behavior, we may similarly infer that the presence of asymmetries of the tower structure along its length affect differently the modes according to the different distribution of displacement along length.

[Figure 9 about here.]

[Figure 10 about here.]

We have yet to acknowledge the origin of the relatively narrow peak on the horizontal components at about 2.3 Hz (Figure 4), at the same time we have not explored torsional motion of the narrow tower. We measure torsion by processing data recorded by two sets of horizontal sensors located at opposite corners of the terrace on the tower top (see Figure 11). After rotating to tangential component and differencing the two parallel components, we find a component proportional to rotation along a vertical axis. The resulting multitaper power spectrum identifies a very clear and narrow peak at 2.3 Hz (Figure 11). Therefore, we can safely identify the peak with the frequency of the (first) torsional mode, slightly shifted in frequency but compatible with predictions from numerical modelling by Invernizzi et al. (2019). The corresponding spectral peak is also present in the spectrum of horizontal translation (Figure 4 at 2.3 Hz). As sensors were placed on the bordering walls, this is well understandable. In this case, amplitude is not maximum at the top

station, as AS97 was not placed along the walls but rather in the roof lantern (Figure 1).

[Figure 11 about here.]

We have so far devoted our attention to horizontal components. The vertical component in not so rich of features, but it can nonetheless be used to detect the mode of axial expansion of the tower along its length. The power spectral densities of records of the 5 stations are shown in Figure 12, where a smooth but clear peak shows at 4.2 Hz. Note that the spectral amplitude is negligible at the base station, and progressively grows with station elevation going to AS35, AS55, AS70, AS97. This is of course consistent with an axial expansion, that we attribute to another mode of free vibration, rather than to the vertical signature of bending in a flexural mode, because it has a different frequency.

[Figure 12 about here.]

Discussion and conclusion

We measure the response of the Asinelli tower to the dynamic input due to vehicular traffic, and verify that this modulated, but essentially continuous, energy source excites many free vibrational modes of the structure. Possible structural damage due to such ceaseless vibrations may need to be evaluated (Nakamura, 1997), however the continual presence of free vibration may allow continuous (passive) monitoring of the properties of the building with simple means, and in turn reveal changes in the state of health of the structure without need for complex setups or analyses (structural health monitoring, Au (2017)). We identify and characterize several flexural modes, as well as an axial compressional and a torsional mode, with a simple and direct analysis based on common seismological tools. They represent parameters that can be used to improve numerical models, and evaluate behavior in case of significant seismic shaking (Riva et al., 1998; Casolo et al., 2013; Valente and Milani, 2016; Palermo et al., 2015; Invernizzi et al., 2019).

Natural frequencies of flexural modes of the Asinelli tower are split into two close principal peaks. Invernizzi et al. (2019) noticed that in realistic finite element models of the

tower the same bending modes occur with slightly different frequencies along two orthogonal directions. We here measure these singlet frequencies, and identify the two principal directions, different for the different modes, that do not align with building figure. It is known that buildings where center of mass and center of stiffness do not coincide, develop a coupled lateral-torsional response (see, e.g., Trombetti and Conte, 2005, and references therein) that identify two, close, different frequencies along the two degrees of freedom. Such structures typically show free vibration responses that, in the time domain, exhibit the characteristic beatings that appear when two close frequencies are superimposed. This phenomenon can be easily observed in the particle motion at the top of the tower (Figure 9). The Asinelli tower is basically a hollow square-base truncated pyramid, but several sources of asymmetry exist. First and most evident is perhaps its inclination. The inclination is due to a rigid rotation of the construction within its foundations, in soft sediments (e.g. Riva et al., 1998), but there are also other factors that may give rise to eccentricities, such as flaws or damage in the construction, that, we recall, dates back to the XII Century and has suffered damages from time, earthquakes and a bombing episode during WWII (e.g., Savioli, 1784; Cavani, 1912; Riva et al., 1998; Palermo et al., 2015; Carpinteri et al., 2016). Invernizzi et al. (2019) elaborate about the need to account for diffused cracking damage, causing anisotropic behavior. The first two flexural modes are rotated with respect to sensor orientation (aligned along cardinal directions) with different angles (Figure 7) with respect to the North. This is also apparent in horizontal particle motion plots (Figure 9, 10). Spectral peaks on the North and East directions for the third mode appears to be independent (Figure 8), hence indicating principal directions aligned with respect to cardinal directions. Structural system identification techniques can be used to derive information on structural properties of a building through the solution of an inverse problem (Au, 2017). However, the differences in behaviour of different modes may also be intuitively understood if we think that modes have different amplitude patterns along the length of the tower (e.g., Figures 5 and 6). They would be mostly affected by any deviation from isotropy, homogeneity and symmetry located where their amplitude is maximum. Hence, as Mordret et al. (2017) also point out, anisotropy, inhomogeneity,

or asymmetry at some specific height would impact different modes differently. This is probably what we are observing. Following this speculation, these data can be important to identify where such defects may be located, and direct focused testing on specific locations.

Our findings support the view that it may be impossible to appropriately reproduce the main parameters of vibration of the tower with dynamical models, without properly accounting for significant deviations from symmetry of the structure, as pointed out by Invernizzi et al. (2019). The analysis of data shows that we are witnessing the effects of deviations from symmetry, homogeneity, or isotropy of structure of the tower — may them be either to defects of construction, weakness of foundations, inclination, or damage. Perhaps such imperfections are distributed at different levels along the length, making a full 3D modelling really necessary. Different location of such heterogeneities would impact the various modes in different ways, because of varying sensitivity of natural modes of vibration to material properties along the length — similarly to what sensitivity kernels represent in seismology. We may point out that more detailed seismological studies — such as Kohler et al. (2018)— may in fact contribute to locate and hence identify the major structural flaws in the structure.

Mechanical models for numerical modeling of historical buildings are often weakened by insufficient experimental information (Palermo et al., 2015). We show that a simple seismographic network, and rather moderate operational effort, can promptly identify many dynamical parameters of a tower, recording only the traffic-generated ground noise typical of urban settings in one day of measurements. This had been done before (e.g. Clinton et al., 2006; Azzara et al., 2020; Wu et al., 2021) but we show that abundant and highly detailed information can be extracted with moderate effort to characterize several features of the complex vibration of the tower.

This analysis is simpler for a slender building such as a tower, but can obviously be extended to any shape of building. Description of patterns of vibration of a more complex shape is of course more complicated (Gentile et al., 2019), and may require a larger number of sensors to sketch it completely (even hundreds of them, Sarlo et al., 2018), and prevent

possible spatial aliasing in the representation of modal shapes. The more specifically-targeted techniques of system identification for operational modal analysis (Reynders, 2012) or natural excitation technique to identify the natural frequencies and mode shapes of a linear dynamic system (James et al., 1995) may become useful to fully exploit such datasets (Sarlo et al., 2018; Zhu et al., 2018).

These observations can be used to refine structural parameters used for dynamical modelling (Azzara et al., 2018). It has been shown that waves propagating in buildings can be used to constrain numerical models based on structural drawings (e.g. Kohler et al., 2007). For historical buildings, the case is made more complicated as structural drawings are not available, and because of the possible presence of structural damages occurred during the centuries. Therefore, such an endeavor carries many complications. Seismological approaches could indeed identify and locate structural flaws (e.g., Kohler et al., 2018), but we do not aim to pursue this here, as it is out of scope for this experimental exploratory study. A simple preliminary comparison with finite element models based on a priori assumptions on structural and material parameters (Riva et al., 1998; Invernizzi et al., 2019; Baraccani et al., 2020) shows fair agreement, but the rich and detailed information resulting from this analysis requires further extensive work.

We used conventional portable seismographic stations, with relatively large sensor packages that needed to rest on rock ledges. This fact posed a number of constraints in sensor location, but we have been lucky enough to find window sills at appropriate distances along the tower. Use of smaller sensor packages may allow to place them more freely (e.g. Gentile et al., 2015) — and even bolt them to the walls — at positions specifically planned. Accelerometers in modern smartphones have also been successfully tested for use in structural health monitoring (Kong et al., 2018) possibly opening new venues for application of inexpensive sensors. However, we show that few high-quality seismometers yield a wealth of information with just a few days of recording.

It has been shown that the signal of Earth's normal modes can be extracted from the background seismic hum (Ventosa et al., 2017). We also have only used background noise as a source of dynamic excitation for this analysis, with the advantage of ease

of operations, repeatability, and possibility to acquire long time series to look for time variations. The engineering community has been using specialized system identification and structural health monitoring techniques for a long time, but we show that classical seismological tools can also provide significant observations with quite simple, convenient, inexpensive, straight, and well-tested procedures.

Data and Resources

Due to their nature, seismographic data used in this publication are not open, but can be made available (under conditions) for specific projects through the contributing author. The electronic supplement to this article contains additional figures S1 and S2 (see text). For seismogram analysis and plotting we used the Seismic Analysis Code – SAC (Goldstein et al., 2003, 2005), available at https://ds.iris.edu/ds/nodes/dmc/software/downloads/sac/. The Multitaper Spectrum Estimation Library (Prieto et al., 2009) is freely available at https://www.gaprieto.com/software. GNU Octave, used for calculating and plotting mode shapes for a cantilevered beam, is free software that can be downloaded from https://www.gnu.org/software/octave/. The original manuscript has been typeset in LaTeX: https://www.latex-project.org.

Author contribution

AM coordinated the project, processed data, prepared plots, and wrote the manuscript. LZ managed the instrumentation loan and contributed to planning, discussion and interpretation. RA calibrated sensors and configured data loggers. RA and AC installed sensors and managed data retrieval, storage, and pre-processing. All authors contributed to field activities, discussed the outcome, and revised the text.

Acknowledgements

We thank the local municipality (*Comune di Bologna*) for interest in the project, for granting us permissions, and for partial financial support. We acknowledge discussions with Dr. Ing. Gilberto Dallavalle, who provided valuable information about the tower. We thank the INGV instrumentation pool for lending us seismometers.

References

Anderson, J. G., P. Bodon, J. Brune, J. Prince, S. Sing, R. Quaas and M. Onate (1986). Strong ground motion from the Michoacan, Mexico, earthquake, *Science* **233** 1043–1049.

Au, S.-K. (2017) Operational Modal Analysis: Modeling, Bayesian Inference, Uncertainty Laws, Springer Nature Singapore Pte Ltd., ISBN 978-981-10-4117-4, DOI 10.1007/978-981-10-4118-1

Azzara R., A. Cavaliere, S. Danesi, A. Morelli, and L. Zaccarelli (2014). Il monitoraggio sismico della Torre degli Asinelli e della Garisenda, Rapporti Tecnici INGV, 284, 1-42, ISSN 2039-7941, http://istituto.ingv.it/images/collane-editoriali/rapporti 20tecnici/rapporti-tecnici-2014/rapporto284.pdf

Azzara RM, De Roeck G, Girardi M, Iafolla V, Padovani C, Pellegrini D and Reynders E (2018) The influence of environmental parameters on the dynamic behaviour of the San Frediano bell tower in Lucca Engineering Structures 156:175-187, doi:10.1016/j.engstruct.2017.10.045

Azzara, R. M., Girardi, M., Iafolla, V., Padovani, C., Pellegrini, D. (2020). Long-Term Dynamic Monitoring of Medieval Masonry Towers . In Frontiers in Built Environment (Vol. 6, p. 9). https://www.frontiersin.org/article/10.3389/fbuil.2020.00009

Backus, G. E., and J. F. Gilbert, 1961. The rotational splitting of the free oscillations of the Earth, Proc. Nat. Acad. Sci., 47, 362-371

448 Baraccani S., R. M. Azzara, G. Gasparini, A. Morelli, M. Palermo, T Trombetti, L. Zac-
449 carelli (2019). Identification through seismometric measurements of transients prop-
450 agating inside the Asinelli and Garisenda towers (Bologna, Italy), implication on
451 structural modeling and state of health monitoring. *7th ECCOMAS Thematic Con-*
452 *ference on Computational Methods in Structural Dynamics and Earthquake Engineer-*
453 *ing, Crete, Greece, 24-26 June 2019, M. Papadrakakis, M. Fragiadakis (eds.)*, doi:
454 10.7712/120119.7193.19071.

455 Baraccani S., Azzara R. M., Palermo M., Gasparini G. and Trombetti T. (2020) Long-
456 Term Seismometric Monitoring of the Two Towers of Bologna (Italy): Modal Frequen-
457 cies Identification and Effects Due to Traffic Induced Vibrations. *Front. Built Environ.*,
458 6:85. doi: 10.3389/fbuil.2020.00085

459 Bernauer F., Wassermann J. M., de Toldi E., Guattari F., Ponceau D., Ripepe M., Igel H.,
460 2017. BlueSeis3A - performance, laboratory tests and applications, S23E-07 presented
461 at 2019 Fall Meeting, AGU, San Francisco, CA, 9-13 Dec.

462 Boutin, C., Hans, S., Ibraim, E., and Roussillon, P. (2005). In situ experiments and seismic
463 analysis of existing buildings. Part II: Seismic integrity threshold. Earthquake Engineer-
464 ing and Structural Dynamics, 34(12), 1531–1546. https://doi.org/10.1002/eqe.503

465 Carpinteri, A., Lacidogna, G., Manuello, A., and Niccolini, G., 2016. A study on the
466 structural stability of the Asinelli Tower in Bologna. Structural Control and Health
467 Monitoring, 23(4), 659–667. DOI: 10.1002/stc.1804

468 Casolo S., G. Milani, G. Uva, C. Alessandri (2013) Comparative seismic vulnerability
469 analysis on ten masonry towers in the coastal Po Valley in Italy, Engineering Structures,
470 49, 465-490.

471 Castellaro S., F. Mulargia, 2010. How far from a building does the ground motion free-
472 field start? The case of thee famous towers and a modern building, Bull. Seismol. Soc.
473 Am., 199, 5A, 2080-2094

474 Cavani F., 1912. Sulla pendenza e sulla stabilità della Torre degli Asinelli di Bologna, R.
475 Accademia delle Scienze dell'Istituto di Bologna, Bologna.

476 Ceccoli, C., Benedetti A., Trombetti T., Silvestri S., Gasparini G., Lometti A., 2014.
477 Valutazione delle caratteristiche dinamiche e sismiche della torre degli Asinelli sita in
478 Bologna, Unpublished manuscript.

479 Chopra, A. K., 2012, Dynamics of Structures: Theory and applications to earthquake
480 engineering, Fourth Edition, Prentice Hall, Upper Saddle River, NJ, ISBN: 0-13-285803-
481 7

482 Chu, Y. C., and Shen, M. H. H. (1992). Analysis of forced bilinear oscillators
483 and the application to cracked beam dynamics. AIAA Journal, 30(10), 2512–2519.
484 https://doi.org/10.2514/3.11254

485 Clinton, J. F., Bradford, S. C., Heaton, T. H., Favela, J. (2006). The Observed Wander
486 of the Natural Frequencies in a Structure. Bull. Seismol. Soc. Am., 96(1), 237-257.
487 https://doi.org/10.1785/0120050052

488 Crowley, H. and Pinho, R., 2010. Revisiting Eurocode 8 formulae for periods of vibration
489 and their employment in linear seismic analysis. Earthquake Engng. Struct. Dyn., 39:
490 223-235. doi:10.1002/eqe.949

491 Deuss, A., Irving, J. C. E., and Woodhouse, J. H., 2010. Regional Variation of Inner Core
492 Anisotropy from Seismic Normal Mode Observations, Science, 328(5981), 1018-1020,
493 doi:10.1126/science.1188596

494 Deuss, A., J. Ritsema, H. van Heijst, 2013. A new catalogue of normal-mode splitting func-
495 tion measurements up to 10 mHz, Geophys. J. Int., 193, 920-937, doi:10.1093/gji/ggt010

496 Dym, C. L., and I. H. Shames, 2013, Solid Mechanics: A Variational Approach, Aug-
497 mented Edition, Springer Science, New York, NY, ISBN: 978-1-4614-6033-6.

498 Dym, C. L., and H. E. Williams, 2007. Estimating fundamental frequencies of tall build-
499 ings. J. of Struct. Engineer., 133(10):1479–1483.

500 Dziewoński, A.M. and Gilbert, F., 1972. Observations of normal modes from 84 recordings
501 of the Alaskan earthquake of 28 March 1964. Geophys. J. R. Astron. Soc., 27, 393-446.

502 Dziewoński, A.M.and Gilbert, F., 1973. Observations of normal modes from 84 recordings
503 of the Alaskan earthquake of 28 March 1974,Part II: spheroidal overtones. Geophys. J.
504 R. Astron. Soc.,35: 401-437.

505 Ekström, G., M. Nettles, and A. M. Dziewoński, 2012, The global CMT project 2004-2010:
506 Centroid-moment tensors for 13,017 earthquakes, Phys. Earth Planet. Int., 200-201, 1-9.

507 Gilbert, F., and Dziewoński, A.M., 1975. An application of normal mode theory to the
508 retrieval of structural parameters and source mechanisms from seismic spectra, Philos.
509 Trans. R. Soc. London, Ser. A, 278, 187-269, http://doi.org/10.1098/rsta.1975.0025.

510 Dziewoński, A. M., T. A. Chou, and J. H. Woodhouse, 1981. Determination of earthquake
511 source parameters from waveform data for studies of global and regional seismicity J.
512 Geophys. Res., 86, 2825-2852

513 Gallipoli, M. R., M. Mucciarelli, B. Sket-Motnikar, P. Zupancic, A. Gosar, S. Prevolnik,
514 M. Herak, J. Stipcevic, D. Herak, Z. Milutinovic, et al. 2010. Empirical estimates
515 of dynamic parameters on a large set of European buildings. Bulletin of Earthquake
516 Engineering 8:593-607. doi:10.1007/s10518-009-9133-6.

517 Gentile C, Ruccolo A, Canali F (2019) Continuous monitoring of the Milan Cathedral:
518 dynamic characteristics and vibration-based SHM, Journal of Civil Structural Health
519 Monitoring (2019) 9:671-688, https://doi.org/10.1007/s13349-019-00361-8

520 Gentile C., A. Saisi and A. Cabboi (2015) Structural Identification of a Ma-
521 sonry Tower Based on Operational Modal Analysis, International Journal of
522 Architectural Heritage: Conservation, Analysis, and Restoration, 9:2, 98-110,
523 doi:10.1080/15583058.2014.951792

524 Goldstein, P., D. Dodge, M. Firpo, Lee Minner (2003) *SAC2000: Signal processing and*
525 *analysis tools for seismologists and engineers, Invited contribution to 'The IASPEI In-*

ternational Handbook of Earthquake and Engineering Seismology', Edited by WHK Lee, H. Kanamori, P.C. Jennings, and C. Kisslinger, Academic Press, London.

Goldstein, P., A. Snoke, (2005), *SAC Availability for the IRIS Community*, Incorporated Institutions for Seismology Data Management Center Electronic Newsletter.

Graney C. M., 2012, Anatomy of a fall: Giovanni Battista Riccioli and the story of g, Physics Today, 9, 36-40, doi:10.1063/PT.3.1716

Guéguen P., P-Y. Bard, and C. S. Oliveira (2000) Experimental and Numerical Analysis of Soil Motions Caused by Free Vibrations of a Building Model, Bull. Seismol. Soc. Am., 90, 6, pp. 1464–1479.

P. Guéguen, P-Y Bard, and F.J. Chávez-García (2002) Site-City Seismic Interaction in Mexico City–Like Environments: An Analytical Study, Bull. Seismol. Soc. Am., Vol. 92, No. 2, pp. 794–811.

He, X., and Tromp, J. (1996), Normal-mode constraints on the structure of the Earth, J. Geophys. Res., 101(B9), 20053- 20082, doi:10.1029/96JB01783.

Invernizzi S., G. Lacidogna, N. E. Lozano-Ramírez, and A., Carpinteri, 2019. Structural monitoring and assessment of an ancient masonry tower, Eng. Fracture Mech., 210, 429-443, doi:10.1016/j.engfracmech.2018.05.011

James III, G. H., Carne, T. G., and Lauffer, J. P. (1995). The natural excitation technique (NExT) for modal parameter extraction from operating structures. International Journal of Analytical and Experimental Modal Analysis, 10(n4), 260-277.

Jennings, P. C., 1970. Distant motions from a building vibration test, Bull. Seismol. Soc. Am., 60, 2037-2043.

Kaya, Y., and E. Şafak. 2015. Real-time analysis and interpretation of continuous data from structural health monitoring (SHM) systems. Bulletin of Earthquake Engineering 13:917-34. doi:10.1007/s10518-014-9642-9.

551 Kohler, M. D., T. H. Heaton, and S. C. Bradford (2007). Propagating waves in the steel,
552 moment-frame Factor building recorded during earthquakes, Bull. Seismol. Soc. Am.
553 97, 1334-1345.

554 Kohler, M. D., Allam, A., Massari, A., and Lin, F. C. (2018). Detection of building
555 damage using helmholtz tomography. Bull. Seismol. Soc. Am., 108(5), 2565–2579.
556 https://doi.org/10.1785/0120170322

557 Kong Q., R. M. Allen, M. Kohler, T. H. Heaton, and J. Bunn, 2018. Structural Health
558 Monitoring of Buildings Using Smartphone Sensors, Seismol. Res. Lett., 89, 594-602,
559 doi:10.1785/0220170111

560 Mantovani R., 2019. Before Foucault: the proofs of the Earth's rotation, Transversal: Int.
561 J. for the Historiography of Science, 7, 58-69, DOI: 10.24117/2526-2270.2019.i7.05

562 Masters, G.; Woodhouse, J.H.; Gilbert, F. (2011), Mineos v1.0.2
563 [software], Computational Infrastructure for Geodynamics, url:
564 https://geodynamics.org/cig/software/mineos/

565 Milani G., S. Casolo, A. Naliato and A. Tralli, 2012. Seismic Assessment of a Medieval Ma-
566 sonry Tower in Northern Italy by Limit, Nonlinear Static, and Full Dynamic Analyses,
567 International Journal of Architectural Heritage: Conservation, Analysis, and Restora-
568 tion, 6:5, 489-524

569 Mordret, A., Sun, H., Prieto, G. A., Toksöz, M. N., Büyüköztürk, O., 2017, Continuous
570 Monitoring of High-Rise Buildings Using Seismic Interferometry, Bull. Seismol. Soc.
571 Am., 107, 6, 2759-2773, doi:10.1785/0120160282.

572 Mucciarelli M., Gallipoli M.R., Ponzo F., Dolce M. (2003) Seismic waves generated by os-
573 cillating buildings: analysis of a release test, Soil Dynamics and Earthquake Engineering
574 23 (2003) 255–262, doi:10.1016/S0267-7261(03)00021-6

575 Murray-Bergquist, L., Bernauer, F., and Igel, H. (2021). Characterization of Six-

576 Degree-of-Freedom Sensors for Building Health Monitoring. Sensors, 21(11), 3732.
577 https://doi.org/10.3390/s21113732

578 Nakata N., R. Snieder, S. Kuroda, S. Ito, T. Aizawa and T. Kunimi (2013) Monitoring
579 a Building Using Deconvolution Interferometry. I: Earthquake-Data Analysis , Bull.
580 Seismol. Soc. Am., 103, 3, 1662-1678.

581 Nakata N., and R. Snieder (2013) Monitoring a Building Using Deconvolution Interfer-
582 ometry. II: Ambient Vibration Analysis, Bull. Seismol. Soc. Am., 104, 1, 204-213.

583 Nakamura, Y. (1997). Seismic Vulnerability Indices for Ground and Structures using
584 Microtremor, World Congress on Railway Research in Florence, Italy.

585 Peeters, B., and G. De Roeck. 1999. Reference-based stochastic subspace identification for
586 output-only modal analysis. Mechanical Systems and Signal Processing 13 (6):855-78.
587 doi:10.1006/mssp.1999.1249.

588 Palermo M., S. Silvestri, G. Gasperini, S. Baraccani, and T. Trombetti, 2015. An ap-
589 proach for the mechanical characterisation of the Asinelli Tower (Bologna) in presence
590 of insufficient experimental data, Journal of Cultural Heritage 16 (2015) 536-543

591 Prieto, G. A., R. L. Parker, F. L. Vernon. (2009), A Fortran 90 library for multita-
592 per spectrum analysis, Computers and Geosciences, 35, pp. 1701-1710. doi:10.1016/
593 j.cageo.2008.06.007.

594 Prieto G. A., J. F. Lawrence, A. I. Chung, and M. D. Kohler (2010) Impulse Response of
595 Civil Structures from Ambient Noise Analysis, Bull. Seismol. Soc. Am., Vol. 100, No.
596 5A, pp. 2322-2328

597 Reynders E. (2012) System identification methods for (operational) modal analysis: re-
598 view and comparison, Arch. Comput Methods Eng.,;19:51–124.

599 Ritsema, J., A. Deuss, H. J. van Heijst, J. H. Woodhouse, 2011. S40RTS: a degree-40
600 shear-velocity model for the mantle from new Rayleigh wave dispersion, teleseismic

601 traveltime and normal-mode splitting function measurements, Geophys. J. Int., 184,
602 1223-1236, doi:10.1111/j.1365-246X.2010.04884.x

603 Ritzwoller M., Masters, G., and F. Gilbert, 1986. Observations of anomalous splitting and
604 their interpretation in terms of aspherical structure, J. Geophys., R., 91, 10203-10228.

605 Riva P., F. Perotti, E. Guidoboni and E. Boschi (1998) Seismic analysis of the Asinelli
606 Tower and earthquakes in Bologna, Soil Dynamics and Earthquake Engineering, 17,
607 525-550

608 Sarlo R., P. A. Tarazaga, and M. E. Kasarda (2018) High resolution operational modal
609 analysis on a five-story smart building T under wind and human induced excitation,
610 Engineering Structures, 176, 279-292, doi:10.1016/j.engstruct.2018.08.060

611 Savioli L. V., 1784. Annali Bolognesi, Vol. 3, Giuseppe Remondini e figli, Bassano.

612 Snieder R. and E. Şafak (2006) Extracting the Building Response Using Seismic Interfer-
613 ometry: Theory and Application to the Millikan Library in Pasadena, California, Bull.
614 Seismol. Soc. of Am., 96, 2, 586-598.

615 Taranath, B. S., 2012. Structural analysis and design of tall buildings, CRC Press, Boca
616 Raton, FL, USA, ISBN 9781439850893.

617 Thomson, D.J., 1982. Spectrum estimation and harmonic analysis. In: Proceedings of the
618 IEEE, vol. 70, pp. 1055–1096.

619 Thompson D., and R. Snieder, 2006. Seismic anisotropy of a building, The Leading Edge,
620 25, 1093, doi:10.1190/1.2349815

621 Trifunac M. D. , S. S. Ivanovic, and M. I. Todorovska (2001a) Apparent periods of a
622 building. I: Fourier Analysis, J. of Struct. Engineer., 127, 5, 517-526.

623 Trifunac M. D. , S. S. Ivanovic, and M. I. Todorovska (2001b) Apparent periods of a
624 building. II: Time-Frequency Analysis, J. of Struct. Engineer., 127, 5, 527-537.

625 Trombetti T. L., and J. P. Conte, 2005. New insight into and simplified approach to seismic
626 analysis of torsionally coupled one-story, elastic systems, J. Sound and Vibration, 286,
627 265-312, doi:10.1016/j.jsv.2004.10.021

628 Valente M., and G. Milani (2016) Seismic assessment of historical masonry towers by
629 means of simplified approaches and standard FEM, Construction and Building Materi-
630 als, 108, 74-104, doi:10.1016.conbuildmat.2016.01.025

631 Ventosa, S., M. Schimmel, and E. Stutzmann, 2017. Extracting surface waves, hum and
632 normal modes: time-scale phase-weighted stack and beyond, Geophys. J. Int., 211,
633 30-44, doi:10.1093/gji/ggx284

634 Wessel, P. and W. H. F. Smith (1998). New, improved version of the Generic Mapping
635 Tools released, *Eos Trans. AGU* **79** 579.

636 van Wijk, K., and S. Hitchman, 2017. Apple seismology, Physics Today, 70, 10, 94,
637 doi:10.1063/PT.3.3740.

638 Woodhouse, J. H., D. Giardini, and X. D. Li, 1986. Evidence for inner core anisotropy
639 from free oscillations, Geophys. Res. Let., 13, 1549-1552.

640 Wu X., Z. Guo, Lanbo Liu, Y. J. Chen, C. Zou, X. Song (2021) Seismic Monitoring of
641 Super High-Rise Building Using Ambient Noise with Dense Seismic Array, Seismol. Res.
642 Let.; 92 (1): 396-407. doi:10.1785/0220200119

643 Zhu Y.-C., Y.-L. Xie, S.-K. Au (2018) Operational modal analysis of an eight-storey
644 building with asynchronous data incorporating multiple setups, Engineering Structures,
645 165, 50-62, doi:10.1016/j.engstruct.2018.03.011

Andrea Morelli [(1)]

Lucia Zaccarelli

Adriano Cavaliere

Istituto Nazionale di Geofisica e Vulcanologia — Sezione di Bologna

Via Marcantonio Franceschini 31, 40135 Bologna, Italy

[(1)] andrea.morelli@ingv.it

Riccardo M. Azzara

Istituto Nazionale di Geofisica e Vulcanologia — Sezione Roma 1

Osservatorio di Arezzo, Via Francesco Redi 13, 52100 Arezzo, Italy

List of Figures

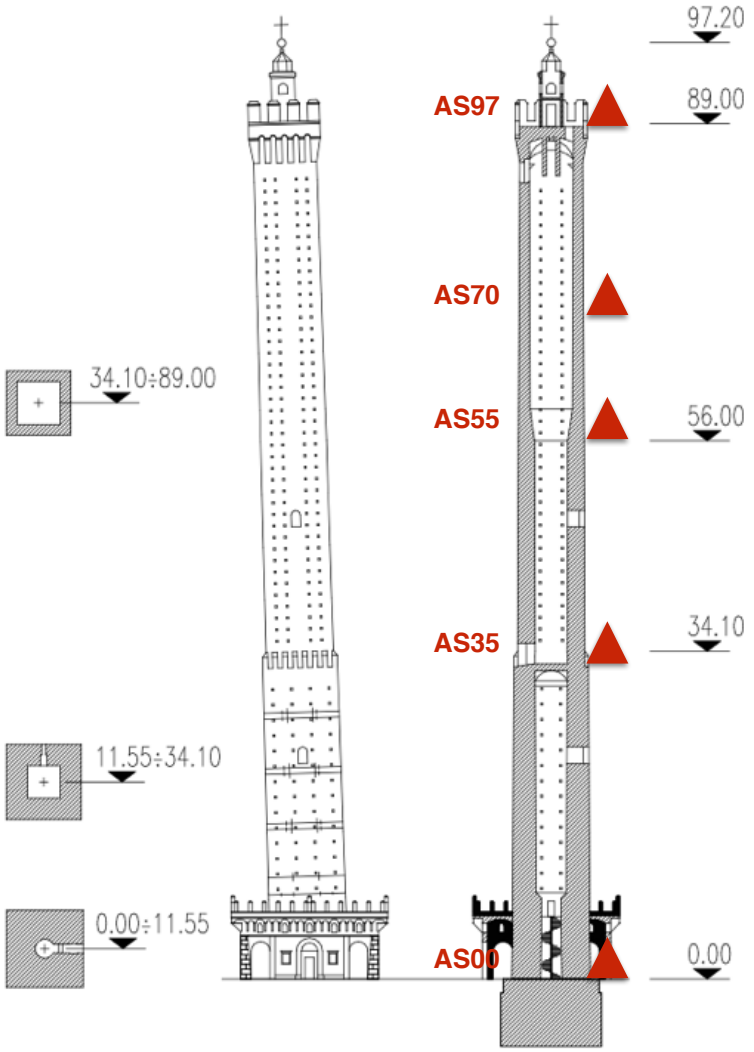

Figure 1: Sketch of the Tower of the Asinelli and, to the right, a cross section. Seismometers had been placed at levels marked by red triangles, labeled by station codes. Black numbers represent height measures in meters above the street level. Floor plans, at left, show the thickness of walls decreasing with height. Wall construction is rubble masonry for the sections up to 56 m height, and solid bricks for the thinner top-section walls. (Modified after G. Dallavalle, personal communication.)

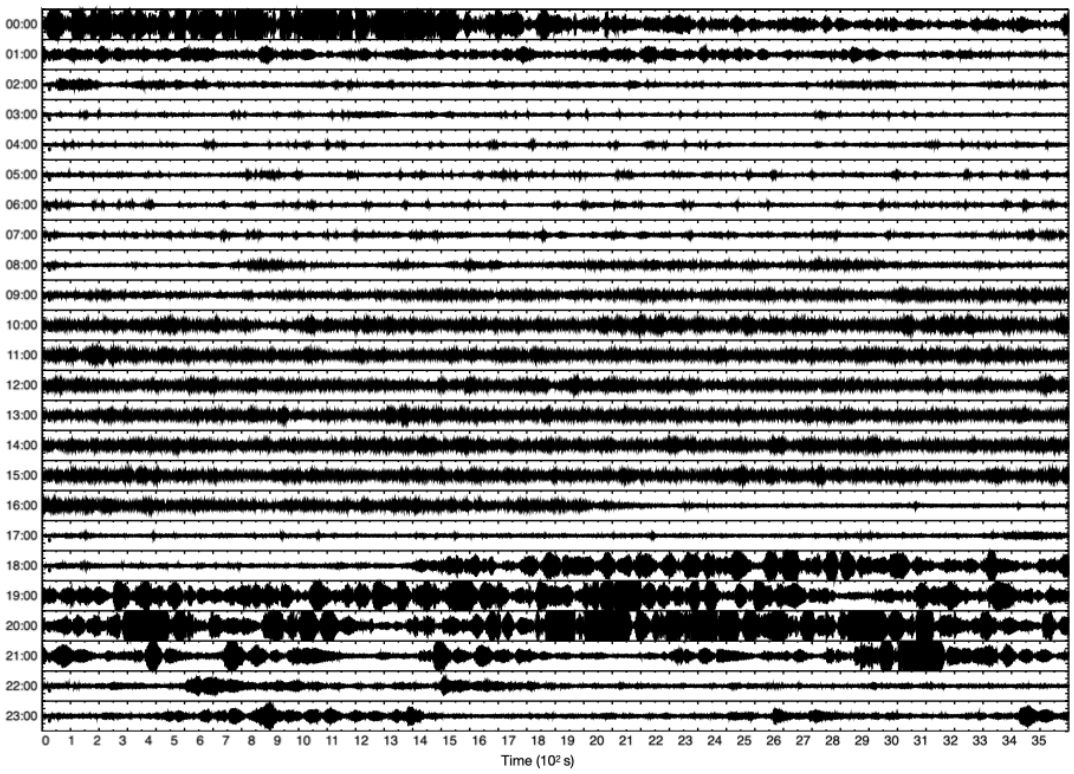

Figure 2: Unfiltered velocity record for one day (Saturday, February 8, 2014) of the North component of station AS97, located at the top of the tower. Each of the 24 traces (normalised to $\pm 2 \cdot 10^{-3}$ m s^{-1}) refers to one full hour, starting from 0:00 and then continuing (as indicated by the trace label to the left), from the top to the bottom trace, until 24:00.

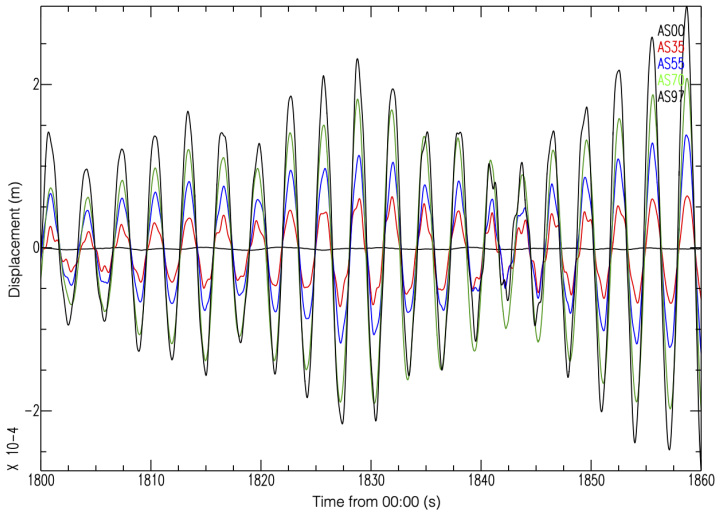

Figure 3: Unfiltered displacement record for one minute of the same day of Figure 2, of the North component of stations at different elevation. Time in seconds from 00:00 of February 8, 2014; displacement in m. The base station, AS00, is plotted in black and, at this scale, looks almost flat (it is the line at 0). Stations at higher elevation (AS35, AS55, AS70, AS97, shown in different colors) progressively show higher amplitudes but always remain in phase. This pattern depicts resonance of the tower with period approximately 3 s, triggered by traffic noise at the base.

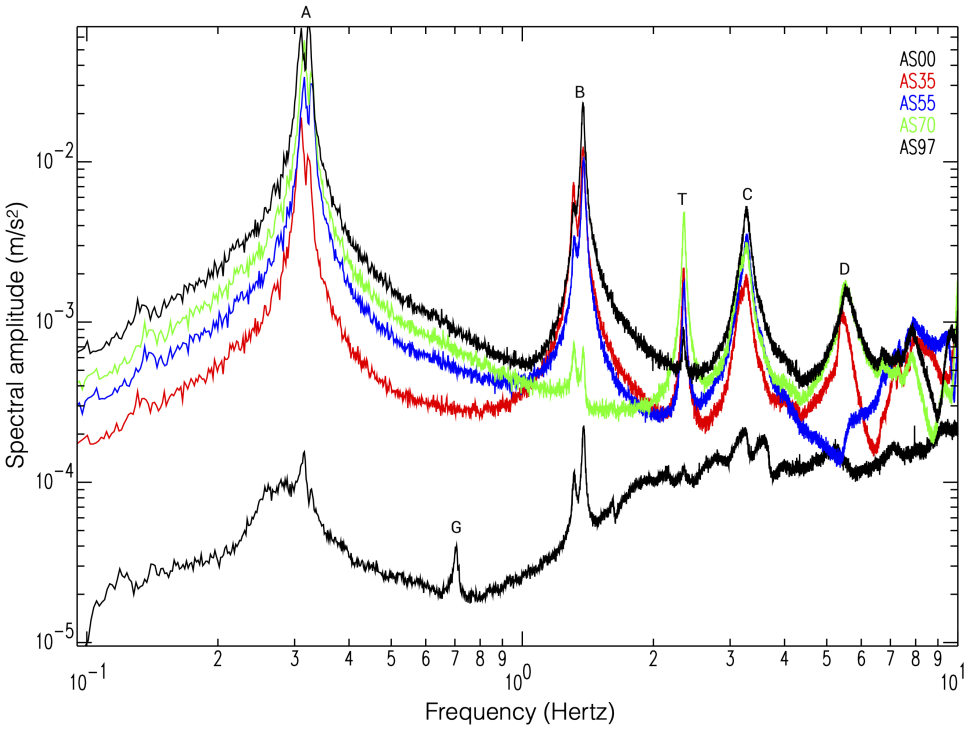

Figure 4: Amplitude spectra of ground acceleration for stations at 5 altitude levels. Average of 10-minute intervals for one day of data. North-oriented horizontal component (East is similar). Different stations are shown with different colors, in turn black, red, blue, green, black for stations AS00, AS35, AS50, AS70, AS97. Peaks labelled by letters (A, B, C, D, T, G) are discussed in the text. The main peak (A) at about 0.32 Hz corresponds to the main resonance visible in the time series of Figure 3. The peak labelled G corresponds to the fundamental mode of sister tower Garisenda.

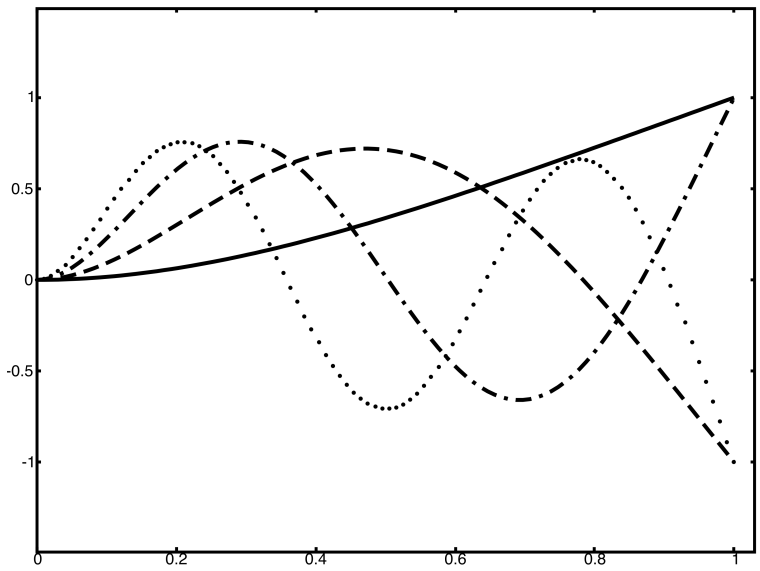

Figure 5: Fundamental vibrational mode (continuous line), first overtone (dashed line), second overtone (dash-dotted line), and third overtone (dotted line) for a uniform cantilevered beam, according to equation 1 (normalised units).

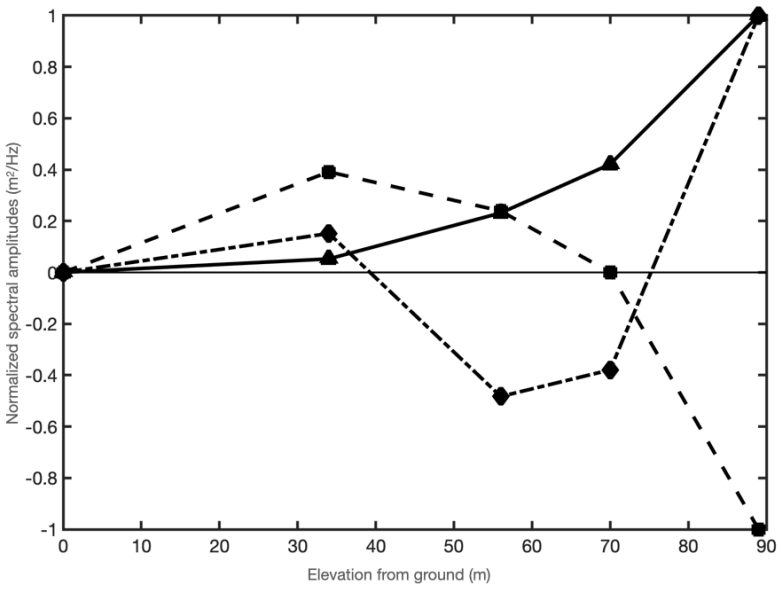

Figure 6: Amplitudes of motion of first three flexural modes, recorded by the 5 seismographic stations. Maximum amplitude is normalised to 1 for each mode for plotting purposes (they span 2 orders of magnitude). Signs are arbitrarily assigned for graphic purposes, assuming no nodal point for mode 1, one nodal point for mode 2, two nodal points for mode 3. Solid triangles connected by continuous line: mode 1. Solid squares connected by dashed line: mode 2. Solid diamonds connected by point-dashed line, mode 3.

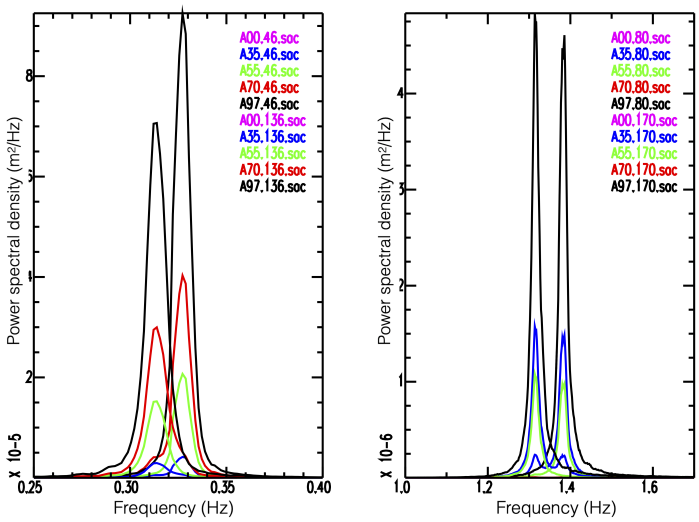

Figure 7: Spectral peaks for the two gravest modes of oscillation: fundamental mode (left panel) and first overtone (right panel). This is power spectral density from multitaper analysis. Spectra have been calculated for rotated directions to isolate single peaks referring to the two principal directions $46^\circ - 136^\circ$ for the fundamental mode (left panel) and $80^\circ - 170^\circ$ for the first overtone (right panel). Spectra for the different stations are plotted with different colors. Note the different amplitudes, as shown in Figure 6. Station AS00, located on the ground, is not visible because of small amplitude.

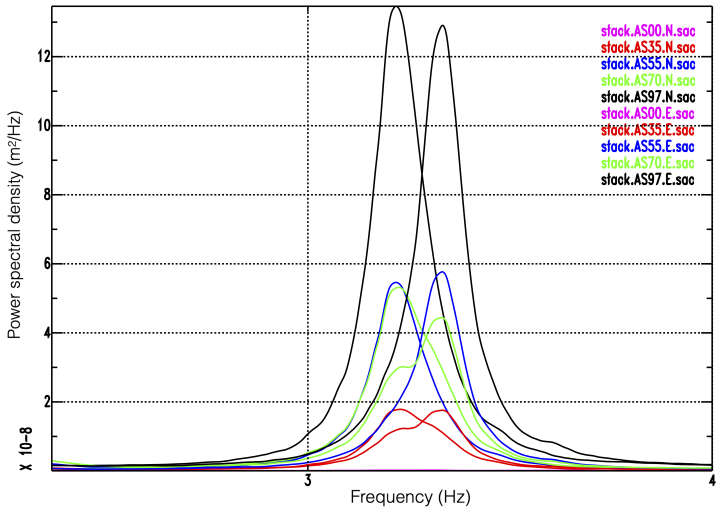

Figure 8: Spectral peaks for the the third mode of oscillation. This is power spectral density from multitaper analysis. Spectra for North and East directions and all stations are superimposed.

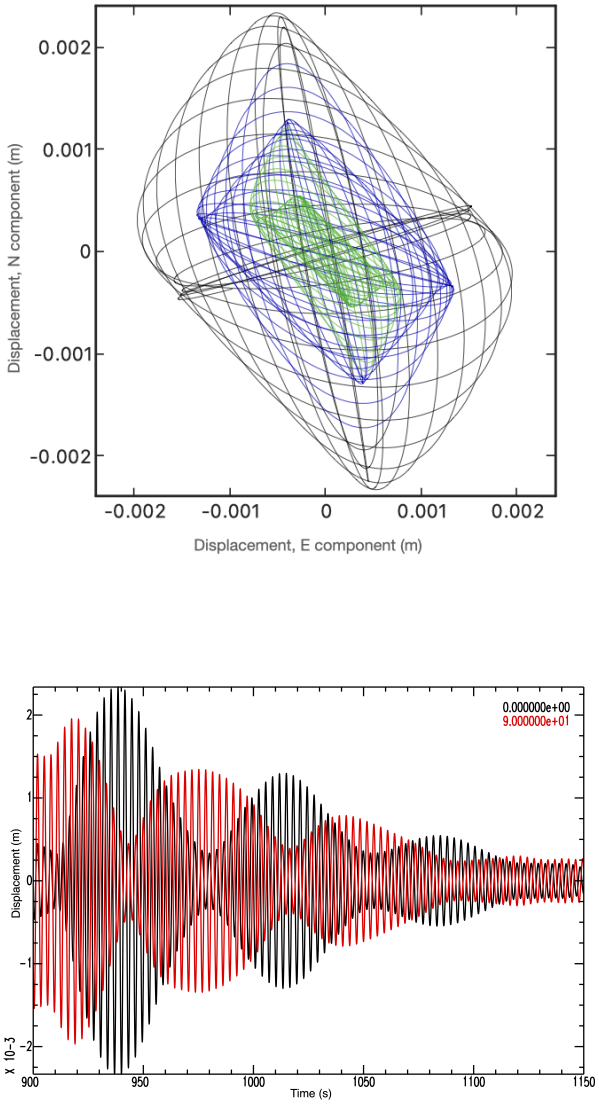

Figure 9: Top: Particle motion on the horizontal plane related to the fundamental mode. Components N, E of station AS97 located at the top of the tower filtered in the frequency band $0.25 \div 0.40\ Hz$. Principal directions at 46° and 136° are apparent. Colors identify consecutive time intervals: black, 0-50s from trace beginning; blue: 50-100s; green: 100-200s. Bottom: displacement along the two principal directions, for the filtered signal for the fundamental mode.

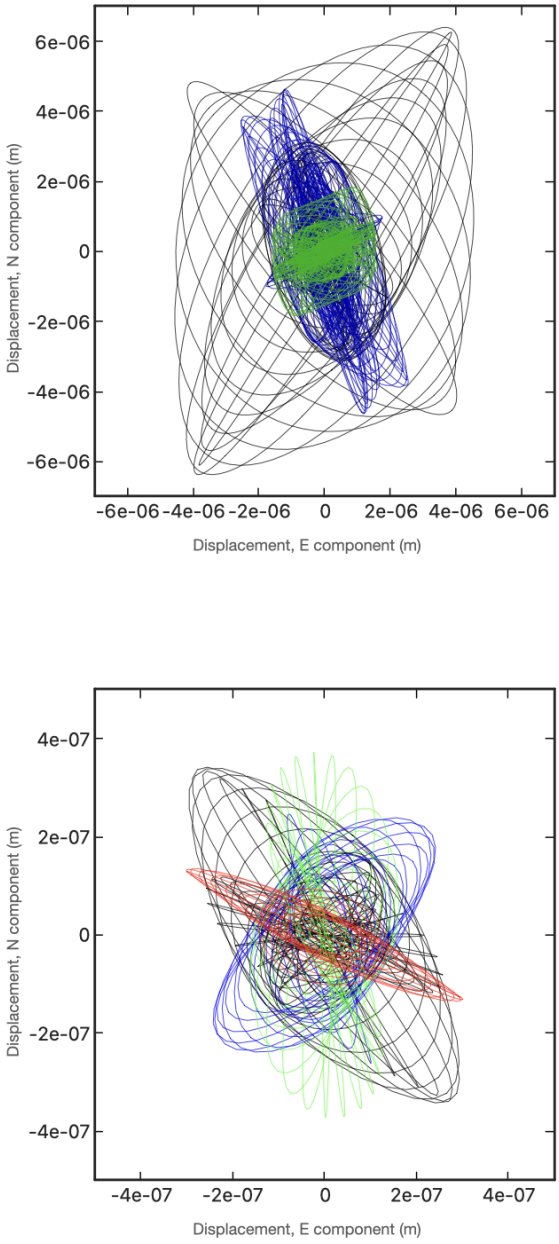

Figure 10: Particle motion on the horizontal plane related to the second (top, filtered in the band $1.1 \div 1.6\ Hz$) and third mode (bottom, $2.5 \div 4.0\ Hz$). Components N, E of station AS97 located at the top of the tower. Displacement follows patterns distinctly different for the different modes. Colors identify consecutive time intervals: black, 0-50s from trace beginning; blue: 50-100s; green: 100-200s for the top panel; black, 0-15s; blue: 15-20s; green: 20-25s; red: 25-30s for the bottom panel.

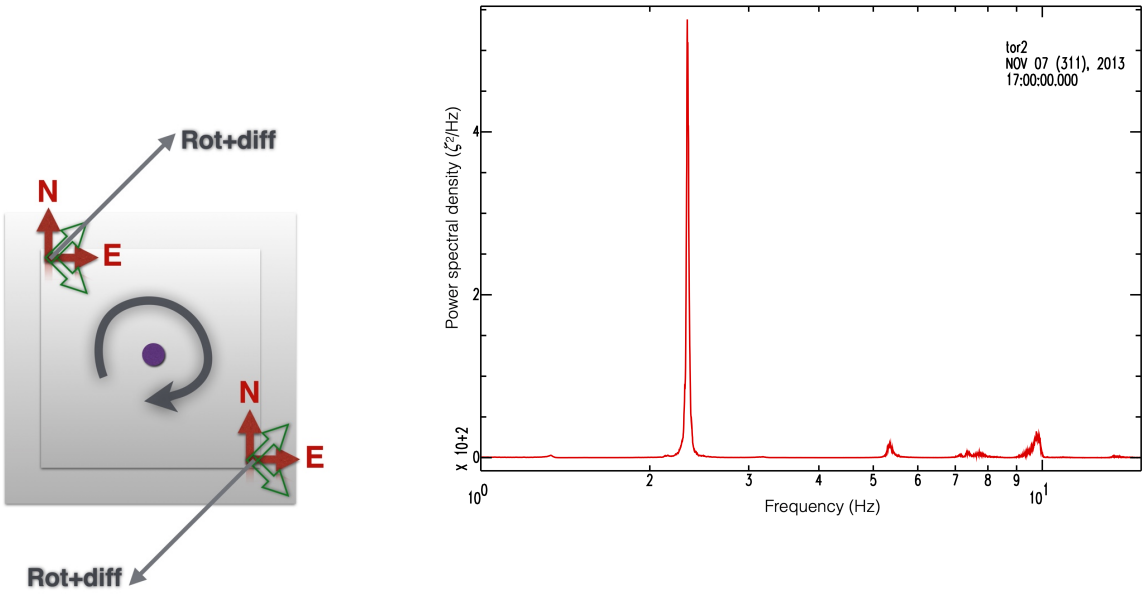

Figure 11: Left: sensor setup to measure rotation on top of the Asinelli tower. Right: multitaper power spectral density of the resulting tangential motion, proportional to rotation ζ (arbitrary units). The narrow peak at about 2.3 Hz corresponds to the fundamental torsional mode.

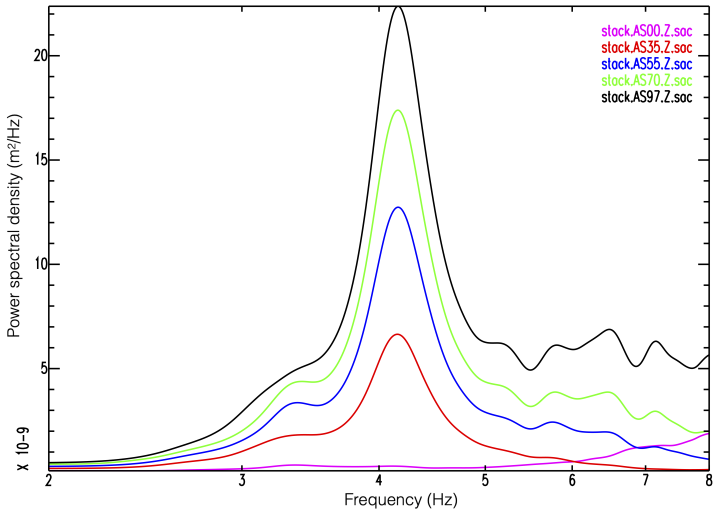

Figure 12: Power spectral density from multitaper analysis of vertical-component data, showing the frequency of axial mode.